

A Meshless Regularization Method for a Two-Dimensional Two-Phase Linear Inverse Stefan Problem

B. Tomas Johansson^{1,*}, Daniel Lesnic² and Thomas Reeve³

¹ Department of Science and Technology, Campus Norrköping, Linköping University, Sweden

² Department of Applied Mathematics, University of Leeds, Leeds LS2 9JT, UK

³ School of Mathematics, University of Birmingham, Birmingham B15 2TT, UK

Received 4 January 2013; Accepted (in revised version) 19 April 2013

Available online 6 September 2013

Abstract. In this paper, a meshless regularization method of fundamental solutions is proposed for a two-dimensional, two-phase linear inverse Stefan problem. The numerical implementation and analysis are challenging since one needs to handle composite materials in higher dimensions. Furthermore, the inverse Stefan problem is ill-posed since small errors in the input data cause large errors in the desired output solution. Therefore, regularization is necessary in order to obtain a stable solution. Numerical results for several benchmark test examples are presented and discussed.

AMS subject classifications: 35K05, 35A35, 65N35, 80A22

Key words: Heat conduction, method of fundamental solutions (MFS), inverse Stefan problem, two-phase change.

1 Introduction

Heat conduction Stefan problems with phase change in multiple dimensions are of importance in several industrial applications in continuous casting of steel, welding processes, crystal and biofilm growth, etc. The classical direct Stefan problem which requires determining both the temperature and the free boundary can become tedious and complicated in the case of multi-dimensional multi-phase models. This fact has motivated researchers to consider inverse Stefan problems in which the free boundary is known and the boundary and/or initial data are unknown [4, 6]. This inverse problem which has application in the technology of refining a material by means of recrystallisation [16],

*Corresponding author.

Email: tomas.johansson@liu.se (B. T. Johansson), amt5ld@maths.leeds.ac.uk (D. Lesnic), reeve@maths.bham.ac.uk (T. Reeve)

is difficult to solve since, as a non-characteristic Cauchy problem, it is ill-posed [2, 4, 9]. Although there exists an extensive literature on one-phase one- and two-dimensional inverse Stefan problems, the two-dimensional two-phase case has been considerably less examined. Prior to this study, [1] regularized such an inverse and ill-posed problem by means of a convolution equation, but the domain considered in their paper is infinite. In this paper, we develop a meshless regularized numerical method of fundamental solutions (MFS) for solving a two-dimensional two-phase linear inverse Stefan problem. In doing so, we extend the recent meshless method of fundamental solutions proposed in [11, 13] for the one-dimensional two-phase and two-dimensional one-phase inverse linear Stefan problems, respectively, to the two-dimensional two-phase change case. Further applications of the MFS to inverse problems can be found in the survey paper [14].

2 Mathematical formulation

In this section, we extend some of the notation and mathematical setup of [5] from the one-phase to the two-phase situation. Let $l > 0$, $T > 0$ and for $t \in [0, T]$ define the liquid (water) zone

$$\Omega_1(t) = \{(x, y) \in \mathbb{R}^2 \mid 0 < x < s(y, t), 0 < y < 1\},$$

and the solid (ice) zone

$$\Omega_2(t) = \{(x, y) \in \mathbb{R}^2 \mid s(y, t) < x < l, 0 < y < 1\},$$

where the liquid-solid interface $s(y, t) \in (0, l)$ is known and given. The boundaries $\partial\Omega_i(t) = \Gamma_i(t) \cup \Sigma(t)$, where

$$\Sigma(t) = \{(x, y) \in \mathbb{R}^2 \mid x = s(y, t), 0 < y < 1\}$$

and $\Gamma_i(t) = \partial\Omega_i(t) \setminus \Sigma(t)$, for $i=1, 2$. Denote also $\Omega(t) = \Omega_1(t) \cup \Sigma(t) \cup \Omega_2(t)$, so that $\partial\Omega(t) = \Gamma_1(t) \cup \Gamma_2(t)$. The whole solution domain of each piece of the composite bi-material, for $i=1, 2$, are denoted by $\Omega_i = \bigcup_{t \in (0, T]} \Omega_i(t)$, and we observe that the boundary $\partial\Omega_i$ of Ω_i consists of the "bottom"

$$\overline{\Omega_1(0)} = \{(x, y) \in \mathbb{R}^2 \mid 0 \leq x \leq s(y, 0), 0 \leq y \leq 1\},$$

$$\overline{\Omega_2(0)} = \{(x, y) \in \mathbb{R}^2 \mid s(y, 0) \leq x \leq l, 0 \leq y \leq 1\},$$

the "top"

$$\overline{\Omega_1(T)} = \{(x, y) \in \mathbb{R}^2 \mid 0 \leq x \leq s(y, T), 0 \leq y \leq 1\},$$

$$\overline{\Omega_2(T)} = \{(x, y) \in \mathbb{R}^2 \mid s(y, T) \leq x \leq l, 0 \leq y \leq 1\},$$

the interface boundary $\Sigma = \bigcup_{t \in (0, T)} \Sigma(t)$, and the "fixed" boundary $\Gamma_i = \bigcup_{t \in (0, T)} \Gamma_i(t)$. We assume that the interface $s \in (0, l)$ is a known and sufficiently smooth function.

The two-dimensional, two-phase linear inverse Stefan problem requires determining the temperature solutions $u_i \in C^{2,1}(\Omega_i) \cap C^{1,0}(\overline{\Omega_i})$ satisfying the heat equations, for $i=1,2$,

$$\alpha_1 \nabla^2 u_1 = \frac{\partial u_1}{\partial t} \quad \text{in } \Omega_1, \tag{2.1a}$$

$$\alpha_2 \nabla^2 u_2 = \frac{\partial u_2}{\partial t} \quad \text{in } \Omega_2, \tag{2.1b}$$

where $\alpha_i > 0$ is the thermal diffusivity of the conductor Ω_i , along with the continuity boundary conditions at the interface $\overline{\Sigma}$, namely

$$u_1 = u_2 = 0 \quad \text{on } \overline{\Sigma}, \tag{2.2a}$$

$$\frac{\partial s}{\partial t} = -K_1 \frac{\partial u_1}{\partial \nu} + K_2 \frac{\partial u_2}{\partial \nu} \quad \text{on } \overline{\Sigma}, \tag{2.2b}$$

where $K_i > 0$ are some constants depending on the thermal conductivities, densities and latent heat, and ν is the inward unit normal pointing outside the liquid zone Ω_1 , a boundary condition on Γ_2 which can be of Dirichlet (or Neumann) type, say

$$u_2 = f \quad \text{on } \Gamma_2 \tag{2.3}$$

and the initial conditions

$$u_1 = u_1^0 \quad \text{on } \Omega_1(0), \tag{2.4a}$$

$$u_2 = u_2^0 \quad \text{on } \Omega_2(0). \tag{2.4b}$$

Given the input data f, u_1^0 and u_2^0 , the compatibility conditions

$$u_1^0 = u_2^0 = 0 \quad \text{on } \Sigma(0), \tag{2.5a}$$

$$f = u_2^0 \quad \text{on } \Gamma_2(0), \tag{2.5b}$$

for a given interface $s(y,t)$, the problem of determining the temperature and heat flux on Γ_1 is termed a two-dimensional, two-phase linear inverse design Stefan problem. In Fig. 1 we present the solution domain and boundary conditions.

An initial attempt would be to split the two-phase Stefan problem (2.1)-(2.5) into a direct problem for u_2 in Ω_2 followed by a one-phase inverse Stefan problem for u_1 in Ω_1 . More specifically, one can first solve, using for example the MFS presented in [12], the direct well-posed problem for u_2 in Ω_2 given by Eqs. (2.1b), (2.3), (2.4b), (2.5b),

$$u_2 = 0 \quad \text{on } \overline{\Sigma}, \tag{2.6a}$$

$$u_2^0 = 0 \quad \text{on } \Sigma(0), \tag{2.6b}$$

and given $s(y,t)$, to determine

$$\frac{\partial u_2}{\partial \nu} =: q_2 \quad \text{on } \overline{\Sigma}. \tag{2.7}$$

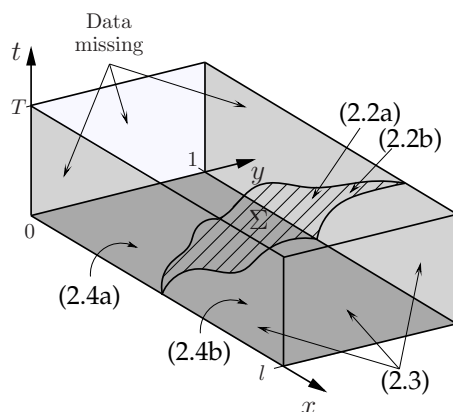


Figure 1: Representation of the two-dimensional two-phase inverse Stefan problem, with locations of the initial and boundary conditions (2.2a)-(2.4).

This output can then be introduced into (2.2b) to yield

$$K_1 \frac{\partial u_1}{\partial \nu} = K_2 q_2 - \frac{\partial s}{\partial t} \quad \text{on } \bar{\Sigma}. \tag{2.8}$$

Then Eqs. (2.1a), (2.4a), (2.8),

$$u_1 = 0 \quad \text{on } \bar{\Sigma}, \tag{2.9a}$$

$$u_1^0 = 0 \quad \text{on } \Sigma(0), \tag{2.9b}$$

for a given interface $s(y,t)$, form a two-dimensional one-phase linear inverse and ill-posed Stefan problem which has been previously solved using the MFS by the authors in [11]. The above splitting is useful in considering the uniqueness of the two-dimensional two-phase inverse Stefan problem (2.1)-(2.5). Namely, the direct problem in Ω_2 given by Eqs. (2.1b), (2.3), (2.4b), (2.5b), (2.6a) and (2.6b) has a unique solution, whilst the two-dimensional one-phase inverse linear Stefan problem given by Eqs. (2.1a), (2.4a), (2.8)-(2.9b) has at most one solution. Moreover, as pointed out in [8], the knowledge of the initial condition (2.4a) with (2.9b) is not needed for obtaining the uniqueness of the solution of the inverse Cauchy-Stefan problem given by Eqs. (2.1a), (2.8) and (2.9a). However, the inverse linear Stefan problem is ill-posed since it may not have a solution even if the surface Σ is analytic [4], and even if the solution does exist, it will not depend continuously on the input data q_2, u_1^0 and s [6]. In this paper, we solve simultaneously, without splitting, the full composite problem (2.1)-(2.5) using the MFS, as described in the next section.

3 The method of fundamental solutions

In this section we combine the MFS of [10] and [11] for the one-dimensional composite and two-dimensional single materials, respectively. We therefore search for a solution

(u_1, u_2) of the problem (2.1)-(2.5) as linear combinations of "non-singular" fundamental solutions, namely

$$u_1(\mathbf{x}, t) = \sum_{m=1}^{2M} \sum_{j=1}^N c_m^{(j)} F_1(\mathbf{x}, t; \mathbf{y}_m^{(j)}, \tau_m), \quad (\mathbf{x}, t) \in \overline{\Omega_1}, \quad (3.1a)$$

$$u_2(\mathbf{x}, t) = \sum_{m=1}^{2M} \sum_{j=1}^N d_m^{(j)} F_2(\mathbf{x}, t; \mathbf{z}_m^{(j)}, \tau_m), \quad (\mathbf{x}, t) \in \overline{\Omega_2}, \quad (3.1b)$$

where

$$F_i(\mathbf{x}, t; \mathbf{x}', t') = \frac{H(t-t')}{4\pi\alpha_i(t-t')} \exp\left(-\frac{|\mathbf{x}-\mathbf{x}'|^2}{4\alpha_i(t-t')}\right), \quad i=1,2, \quad (3.2)$$

are the fundamental solutions of the heat equations (2.1a) and (2.1b) and H is the Heaviside function.

In expressions (3.1a) and (3.1b), the source points $(\mathbf{y}_m^{(j)}, \tau_m)$ and $(\mathbf{z}_m^{(j)}, \tau_m)$ for $m = \overline{1, 2M}$, $j = \overline{1, N}$ are located outside their corresponding solution domains $\overline{\Omega_1}$ and $\overline{\Omega_2}$, respectively. In particular, we take the times $(\tau_m)_{m=\overline{1, 2M}}$ uniformly distributed in $(-T, T)$ as

$$\tau_m = \frac{(2m - 2M - 1)T}{2M}, \quad m = \overline{1, 2M},$$

and the space points $\mathbf{y}_m^{(j)}$ and $\mathbf{z}_m^{(j)}$ on fictitious lateral boundaries $\partial\Omega_1'(t)$ and $\partial\Omega_2'(t)$, which embrace the domains $\Omega_1(t)$ and $\Omega_2(t)$, respectively, where for $t \in [-T, 0)$ we define

$$\begin{aligned} \Omega_1(t) &= \{(x, y) \in \mathbb{R}^2 \mid 0 < x < s(y, -t), \ 0 < y < 1\}, \\ \Omega_2(t) &= \{(x, y) \in \mathbb{R}^2 \mid s(y, -t) < x < l, \ 0 < y < 1\}, \end{aligned}$$

as the mirror images of $\Omega_1(t)$ and $\Omega_2(t)$ for $t \in [0, T]$. At the fixed time $\tau = \tau_m$ we have, [11],

$$\begin{aligned} \mathbf{y}_m^{(j)} &= \begin{cases} \left(s\left(\frac{2j-1}{N/2}, \tau_m\right) + h_1, \frac{2j-1}{N/2} \right), & \text{for } j = \overline{1, N/4}, \\ \left(\frac{s(1, \tau_m)(2(j-N/4)-1)}{N/2}, 1 + h_1 \right), & \text{for } j = \overline{N/4+1, N/2}, \\ \left(-h_1, 1 - \frac{2(j-N/2)-1}{N/2} \right), & \text{for } j = \overline{N/2+1, 3N/4}, \\ \left(\frac{s(0, \tau_m)(2(j-3N/4)-1)}{N/2}, -h_1 \right), & \text{for } j = \overline{3N/4+1, N}, \end{cases} \\ \mathbf{z}_m^{(j)} &= \begin{cases} \left(l + h_2, \frac{2j-1}{N/2} \right), & \text{for } j = \overline{1, N/4}, \\ \left(s(1, \tau_m) + \frac{(l-s(1, \tau_m))(2(j-N/4)-1)}{N/2}, 1 + h_2 \right), & \text{for } j = \overline{N/4+1, N/2}, \\ \left(-h_2 + s\left(\frac{2(3N/4-j)+1}{N/2}, \tau_m\right), \frac{2(3N/4-j)+1}{N/2} \right), & \text{for } j = \overline{N/2+1, 3N/4}, \\ \left(s(0, \tau_m) + \frac{(l-s(0, \tau_m))(2(j-3N/4)-1)}{N/2}, -h_2 \right), & \text{for } j = \overline{3N/4+1, N}. \end{cases} \end{aligned}$$

The parameters $h_1, h_2 > 0$ need to be prescribed and they are characterising the distance between the space boundary of the solution domains, $\overline{\Omega_1}$ and $\overline{\Omega_2}$, respectively, and the exterior dilated space boundaries on which the source points are located. Preliminary and previous experience indicates that h_1 and h_2 should be chosen neither too small nor too large and, in this study, they are chosen by trial and error. Alternatively, in a future work they could be optimized such that the error between the numerical MFS solutions (3.1a,b) and the data on the boundary $\overline{\Sigma} \cup \Gamma_2 \cup \Omega_1(0) \cup \Omega_2(0)$ is minimized (viz maximum principle for the heat equation).

Once we have selected the $2(N \times 2M)$ source points $\mathbf{y}_m^{(j)} \in \cup_{t \in [-T, T]} \partial \Omega_1'(t)$ and $\mathbf{z}_m^{(j)} \in \cup_{t \in [-T, T]} \partial \Omega_2'(t)$, we select the collocation points on $\overline{\Sigma} \cup \Gamma_2 \cup \Omega_1(0) \cup \Omega_2(0)$. Let

$$t_i = \frac{iT}{M_1} \quad \text{for } i = \overline{0, M_1}.$$

At the fixed time $t = t_i$ we define the collocation points

$$\mathbf{x}_k^{(i)} = \left(s \left(\frac{2k-1}{N_1/2}, t_i \right), \frac{2k-1}{N_1/2} \right) \quad \text{for } k = \overline{1, N_1/4}.$$

Collocating the Stefan conditions (2.2a) and (2.2b) at these points, we obtain $3N_1 \times (M_1 + 1)/4$ equations. We also need to impose the initial conditions (2.4a) (if prescribed) and (2.4b). At the time $t = 0$, we take some uniform distribution of points on $\Omega_1(0)$ as

$$\boldsymbol{\omega}_k^{(j)} = \left(\frac{k}{M_2} s(y_j, 0), \frac{j}{N_1/2 + 1} \right) \quad \text{for } k = \overline{1, M_2 - 1}, \quad j = \overline{1, N_1/2},$$

and on $\Omega_2(0)$ as

$$\mathbf{w}_k^{(j)} = \left(s(y_j, 0) + \frac{(l - s(y_j, 0))k}{M_2}, \frac{j}{N_1/2 + 1} \right) \quad \text{for } k = \overline{1, M_2 - 1}, \quad j = \overline{1, N_1/2}.$$

Collocating the initial conditions (2.4a) and (2.4b) at these points we obtain an extra $N_1 \times (M_2 - 1)$ equations.

We finally collocate the boundary condition (2.3) at points on Γ_2 , namely at each t_i for $i = \overline{0, M_1}$

$$\begin{aligned} \mathbf{v}_k^{(1)} &= \left(l, \frac{2k-1}{N_1/2} \right) && \text{for } k = \overline{1, N_1/4}, \\ \mathbf{v}_j^{(2)} &= \left(s(0, t_i) + \frac{(l - s(0, t_i))(2j-1)}{2M_3}, 0 \right) && \text{for } j = \overline{1, M_3}, \\ \mathbf{v}_j^{(3)} &= \left(s(1, t_i) + \frac{(l - s(1, t_i))(2j-1)}{2M_3}, 1 \right) && \text{for } j = \overline{1, M_3}, \end{aligned}$$

to obtain an extra $(N_1/4 + 2M_3) \times (M_1 + 1)$ equations.

Summing up we obtain a linear system of $N_1(M_1 + M_2) + 2M_3(M_1 + 1)$ equations with $4NM$ unknowns. Choosing parameters such that $N_1(M_1 + M_2) + 2M_3(M_1 + 1) \geq 4NM$ we obtain a square or over-determined system of linear equations, say

$$\mathbf{A}\mathbf{X} = \mathbf{B}, \quad (3.3)$$

where

$$\mathbf{X} = (c_m^{(j)}, d_m^{(j)})^{tr} \quad \text{for } m = \overline{1, 2M}, \quad j = \overline{1, N},$$

is the unknown vector of MFS coefficients, A is a matrix containing the values of the fundamental solutions (3.2) and its normal derivatives at the source and collocation points outlined above, and \mathbf{B} is a vector containing the input values of $\partial s / \partial t$, f , u_1^0 and u_2^0 at the respective collocation points.

Since the inverse problem is ill-posed and, in addition, the MFS results in ill-conditioned systems of equations, regularization is necessary [3, 15]. Therefore, instead of solving (3.3) we minimize the functional $\|\mathbf{A}\mathbf{X} - \mathbf{B}\|^2 + \lambda\|\mathbf{X}\|^2$ which yields the regularized solution

$$\mathbf{X}_\lambda = (\mathbf{A}^{tr}\mathbf{A} + \lambda\mathbf{I})^{-1}\mathbf{A}^{tr}\mathbf{B}, \quad (3.4)$$

where \mathbf{I} is the identity matrix, the superscript tr denotes the transpose of the matrix, and $\lambda > 0$ is a regularization parameter to be prescribed by trial and error, or according to some specialized criterion such as the discrepancy principle, the generalized cross validation or the L -curve criterion [7]. By trial and error we mean that we choose the smallest $\lambda > 0$ for which a stable (free of oscillations and unbounded behaviour) numerical solution is still obtained.

4 Numerical results and discussion

In this section we investigate numerically three benchmark test examples of two-dimensional two-phase inverse Stefan problems. The first two examples possess an analytic solution and correspond to the problem given by Eqs. (2.1)-(2.5) in which the initial condition (2.4a) is known. The relative (percentage) error (%) is calculated as

$$\left| \frac{\text{analytic} - \text{numeric}}{\text{analytic}} \right| \times 100.$$

Note that in the first two examples we have not included the relative error along the free boundary $\overline{\Sigma}$, due to the homogeneous interface condition (2.2a). The third example does not have an analytical solution available and moreover, the initial condition (2.4a) is unknown. We take $M_1 = 20$, $M_2 = 20$, $M_3 = 10$, $N_1 = 40$, $M = 10$, $N = 40$, i.e., 2020 collocation points (equations) and 1600 source points (unknowns).

4.1 Example 1

We solve the problem (2.1)-(2.5) with the input data given by $T = 1$, $l = 3$, $\alpha_1 = 1$, $K_1 = 7/(2\sqrt{5})$, $\alpha_2 = 1/2$, $K_2 = 3/\sqrt{5}$. The moving boundary is given by

$$s(y,t) = \frac{y+1}{2} + \frac{5t}{4}, \quad (y,t) \in (0,1) \times (0,1), \quad (4.1a)$$

$$u_2(3,y,t) = \exp\left(-5+y+\frac{5t}{2}\right) - 1, \quad (y,t) \in (0,1) \times (0,1), \quad (4.1b)$$

$$u_2(x,0,t) = \exp\left(-2x+1+\frac{5t}{2}\right) - 1, \quad (x,t) \in (s(0,t),3) \times (0,1), \quad (4.1c)$$

$$u_2(x,1,t) = \exp\left(-2x+2+\frac{5t}{2}\right) - 1, \quad (x,t) \in (s(1,t),3) \times (0,1), \quad (4.1d)$$

$$u_1(x,y,0) = u_1^0(x,y) = \exp\left(-x+\frac{y+1}{2}\right) - 1, \\ (x,y) \in \Omega_1(0) = \{(x,y) \in \mathbb{R}^2 \mid y \in (0,1), x \in (0,s(y,0))\}, \quad (4.1e)$$

$$u_2(x,y,0) = u_2^0(x,y) = \exp(-2x+y+1) - 1, \\ (x,y) \in \Omega_2(0) = \{(x,y) \in \mathbb{R}^2 \mid y \in (0,1), x \in (s(y,0),3)\}. \quad (4.1f)$$

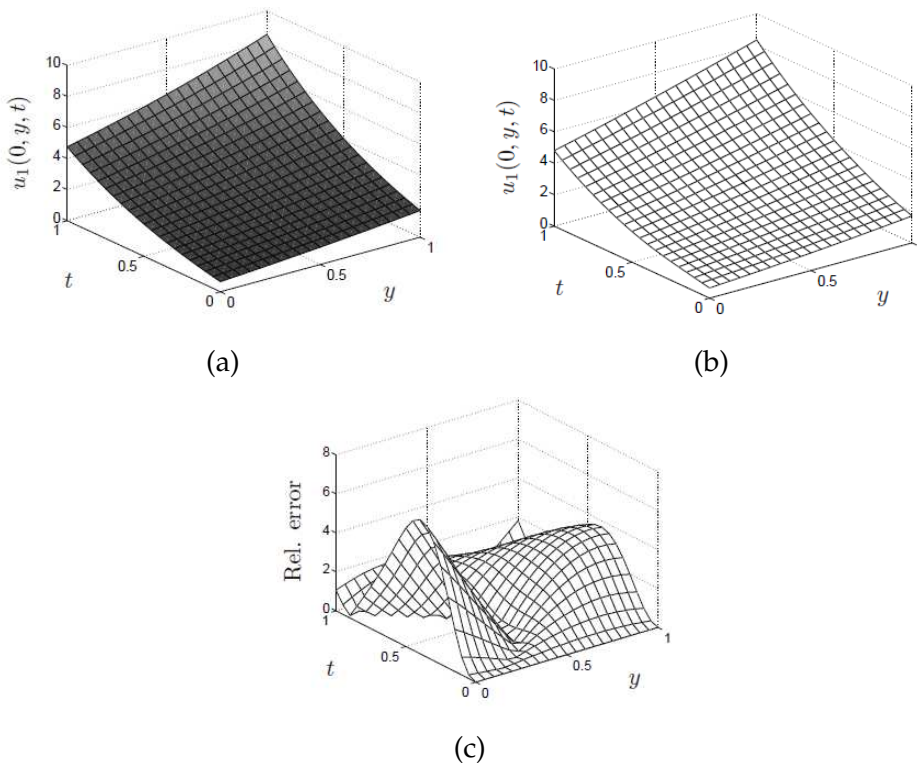


Figure 2: (a) The exact temperature solution, (b) the MFS approximation, and (c) the relative error (%) on the boundary $x=0$, obtained with $h_1=4$ and $h_2=2$, for Example 1 (no noise).

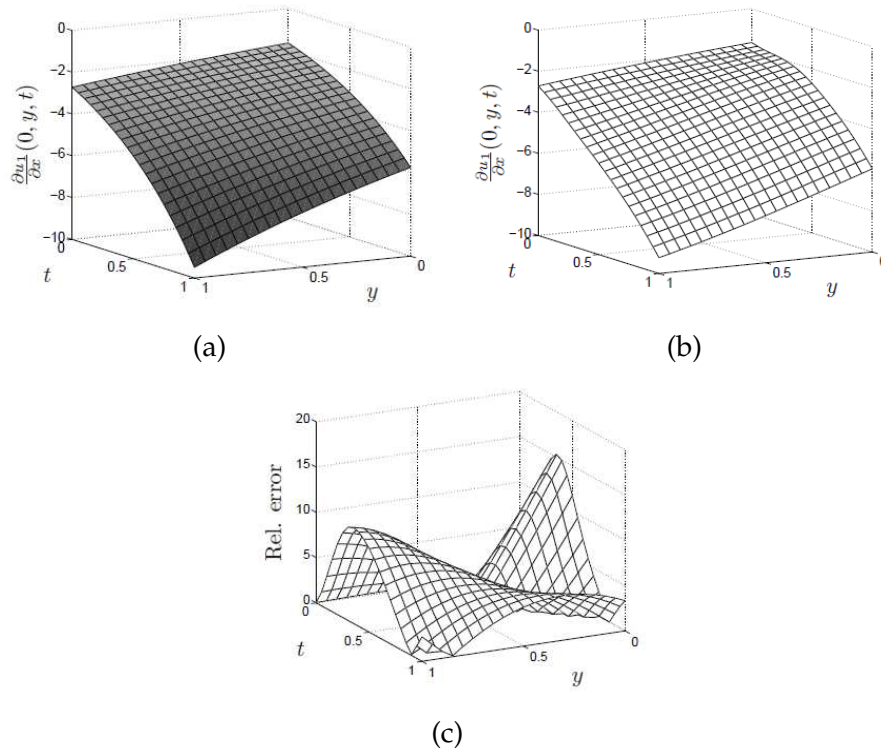


Figure 3: (a) The exact heat flux, (b) the MFS approximation, and (c) the relative error (%), on the boundary $x=0$, obtained with $h_1=4$ and $h_2=2$, for Example 1 (no noise).

Note that the inward unit normal to the interface boundary $\Sigma = \{(x, y, t) \in \mathbb{R}^3 \mid y \in (0, 1), t \in (0, 1), x = s(y, t)\}$ is given by

$$\mathbf{v} = -\frac{\nabla\Phi}{|\nabla\Phi|} = \frac{1}{\sqrt{5/4}} \left(-1, \frac{1}{2}\right),$$

where

$$\Phi(x, y, t) = x - s(y, t).$$

Then the problem given by the Eqs. (2.1)-(2.2b), (4.1a)-(4.1f) has the analytic solution

$$u_1(x, y, t) = \exp\left(-x + \frac{y+1}{2} + \frac{5t}{4}\right) - 1, \quad (x, y, t) \in \bar{\Omega}_1 = \{(x, y, t) \in \mathbb{R}^3 \mid y \in [0, 1], t \in [0, 1], x \in [0, s(y, t)]\}, \quad (4.2a)$$

$$u_2(x, y, t) = \exp\left(-2x + y + 1 + \frac{5t}{2}\right) - 1, \quad (x, y, t) \in \bar{\Omega}_2 = \{(x, y, t) \in \mathbb{R}^3 \mid y \in [0, 1], t \in [0, 1], x \in [s(y, t), 3]\}. \quad (4.2b)$$

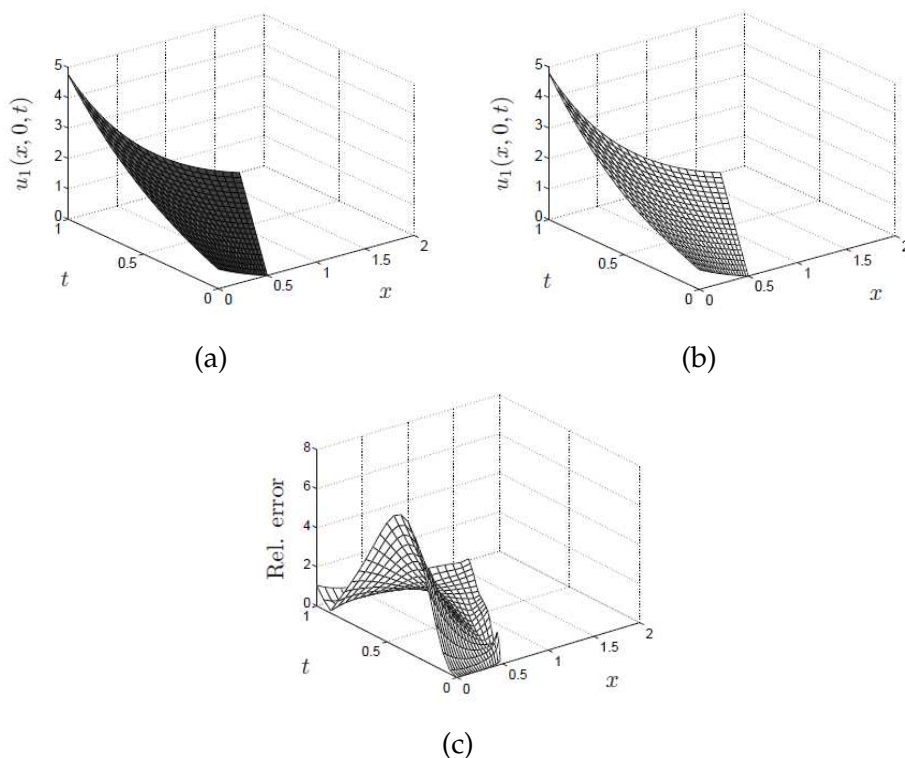


Figure 4: (a) The exact temperature solution, (b) the MFS approximation, and (c) the relative error (%), on the boundary $y=0$, obtained with $h_1=4$ and $h_2=2$, for Example 1 (no noise).

One can check that conditions (2.2a) and (2.2b) are satisfied by direct substitution and using

$$\frac{\partial u_1}{\partial \nu} = \sqrt{5/4}, \quad \frac{\partial u_2}{\partial \nu} = \sqrt{5} \quad \text{on } \bar{\Sigma}.$$

The unknown data which is sought is given by the temperature u_1 on Γ_1 and the heat flux $\partial u_1 / \partial \nu$ on the left wall $x=0$, namely

$$u_1(0, y, t) = \exp\left(\frac{y+1}{2} + \frac{5t}{4}\right) - 1, \quad \frac{\partial u}{\partial x}(0, y, t) = -\exp\left(\frac{y+1}{2} + \frac{5t}{4}\right), \quad (y, t) \in (0, 1) \times (0, 1), \tag{4.3a}$$

$$u_1(x, 0, t) = \exp\left(-x + \frac{1}{2} + \frac{5t}{4}\right) - 1, \quad (x, t) \in (0, s(0, t)) \times (0, 1), \tag{4.3b}$$

$$u_1(x, 1, t) = \exp\left(-x + 1 + \frac{5t}{4}\right) - 1, \quad (x, t) \in (0, s(1, t)) \times (0, 1). \tag{4.3c}$$

In order to test the stability of the numerical results noise is added to the temperature data (2.3), via (4.1b)-(4.1d), as

$$u_2^p = (1 + p\rho)f \quad \text{on } \Gamma_2, \tag{4.4}$$

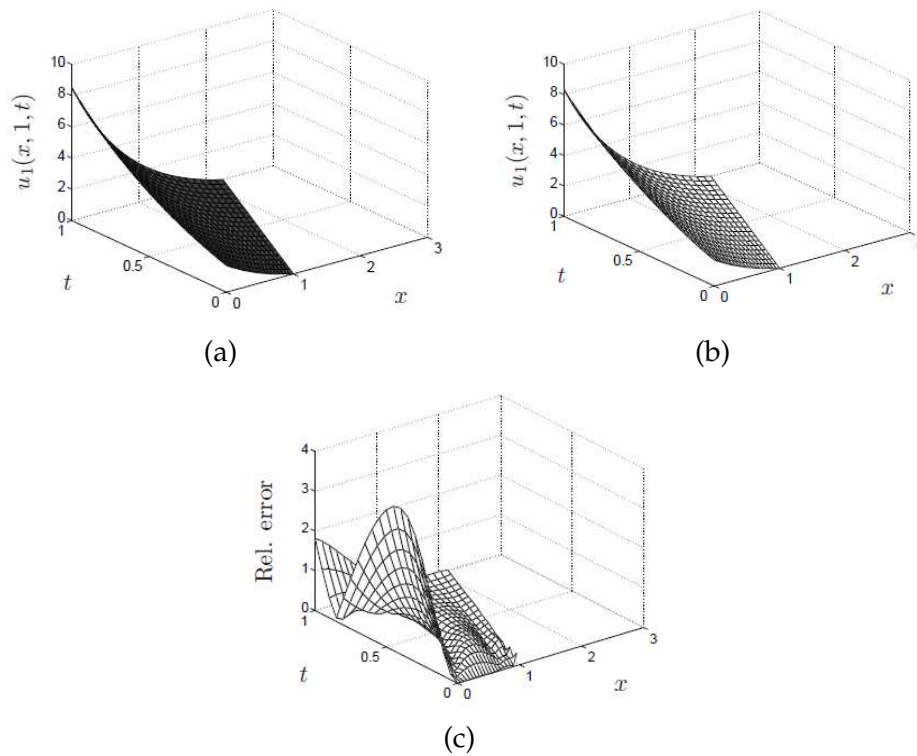


Figure 5: (a) The exact temperature solution, (b) the MFS approximation, and (c) the relative error (%), on the boundary $y=1$, obtained with $h_1=4$ and $h_2=2$, for Example 1 (no noise).

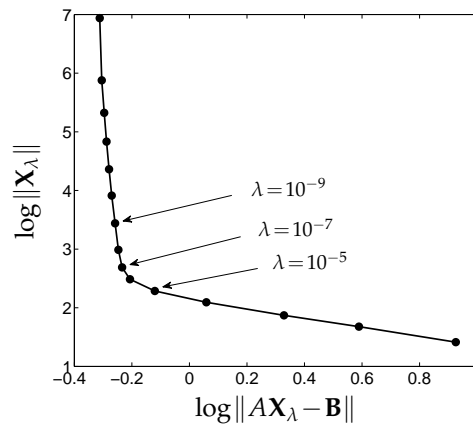


Figure 6: The L -curve for Example 1 ($p=5\%$ noise).

where p is the percentage of noise and ρ are random variables taken from a uniform distribution in $[-1,1]$.

Figs. 2 and 3 show the numerical results for the temperature and the heat flux at the

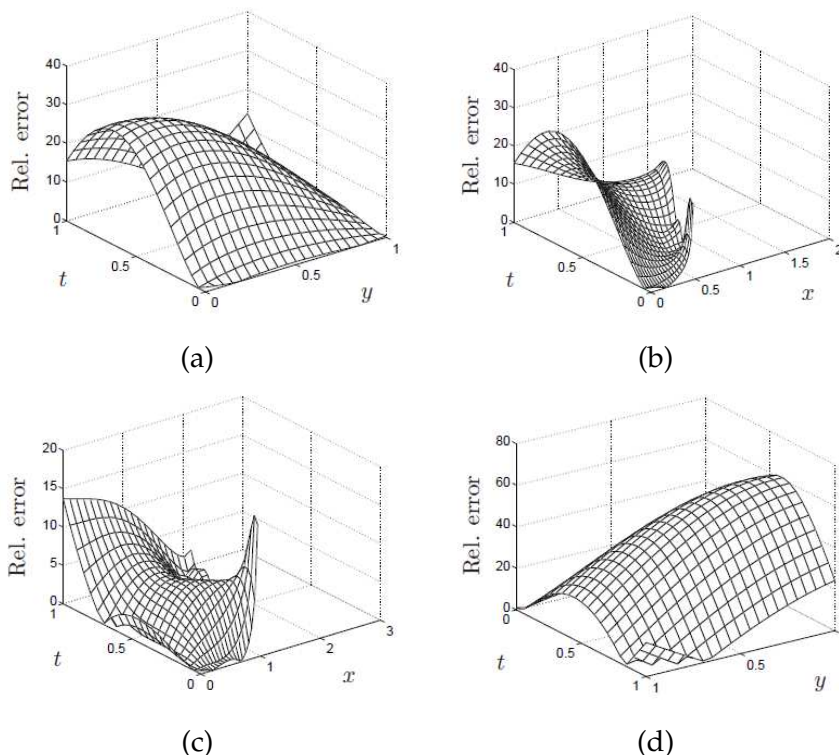


Figure 7: The relative error between the exact and numerical $u_1(x,y,t)$ on (a) $x=0$, (b) $y=0$, (c) $y=1$, and (d) the relative error (%) between the exact and numerical $(\partial u_1 / \partial x)(0,y,t)$, obtained with $h_1=3$ and $h_2=2$, for Example 1 ($p=5\%$ noise).

boundary $x=0$ in comparison with the exact solutions (4.3a) when $p=0$, i.e., when there is no noise in the data (4.4), and $\lambda=10^{-14}$. From these figures it can be seen that the MFS numerical approximations are in good agreement with the exact solution. Additionally, Figs. 4 and 5 show the results for the temperature on the boundaries $y=0$ and $y=1$, respectively, and again the agreement with the exact solutions (4.3b) and (4.3c) is excellent. Next, in order to investigate the stability of the numerical results we add $p=5\%$ noise into the flux data (4.4) and take $\lambda=10^{-7}$. Fig. 6 presents the L -curve which plots the logarithm of the residual $\log \|A\mathbf{X}_\lambda - \mathbf{B}\|$ versus the logarithm of the norm $\log \|\mathbf{X}_\lambda\|$ for various values of $\lambda > 0$. From this figure it can be seen that the corner of the L -curve occurs near $\lambda=10^{-7}$.

Fig. 7 shows the relative error plots and from these it can be seen that the numerical solution is stable and reasonably accurate.

4.2 Example 2

We investigate a similar example to [13], which considered the one-dimensional two-phase linear inverse Stefan problem (and is extended to the two-dimensional case here).

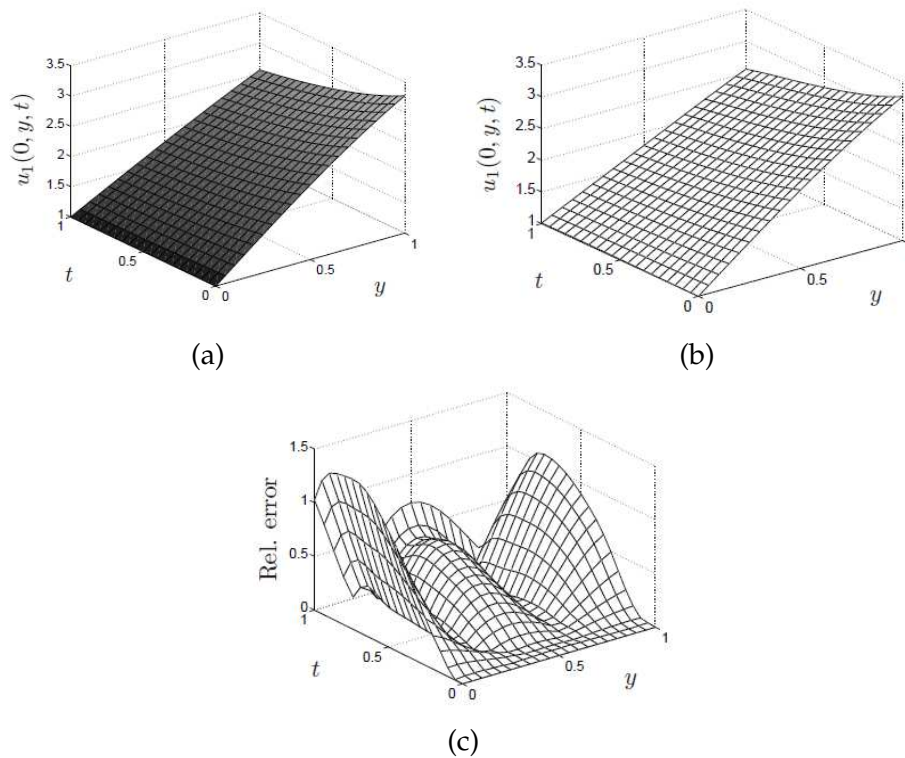


Figure 8: (a) The exact temperature solution, (b) the MFS approximation, and (c) the relative error (%), on the boundary $x=0$, obtained with $h_1=h_2=2$, for Example 2 (no noise).

The input data is given by $T=1, l=2, \alpha_1=0.5, \alpha_2=1, K_1=0.252612$ and $K_2=\sqrt{2}$. The free boundary is given by

$$s(y,t) = \gamma\sqrt{t+t^0} + y, \quad (y,t) \in (0,1) \times (0,1), \tag{4.5}$$

with the boundary data given by

$$u_2(2,y,t) = -1 + \frac{\operatorname{erfc}\left(\frac{2-y}{\sqrt{8\alpha_2(t+t^0)}}\right)}{\operatorname{erfc}\left(\frac{\gamma}{\sqrt{8\alpha_2}}\right)}, \quad (y,t) \in (0,1) \times (0,1), \tag{4.6a}$$

$$u_2(x,0,t) = -1 + \frac{\operatorname{erfc}\left(\frac{x}{\sqrt{8\alpha_2(t+t^0)}}\right)}{\operatorname{erfc}\left(\frac{\gamma}{\sqrt{8\alpha_2}}\right)}, \quad (x,t) \in (s(0,t),2) \times (0,1), \tag{4.6b}$$

$$u_2(x,1,t) = -1 + \frac{\operatorname{erfc}\left(\frac{x-1}{\sqrt{8\alpha_2(t+t^0)}}\right)}{\operatorname{erfc}\left(\frac{\gamma}{\sqrt{8\alpha_2}}\right)}, \quad (x,t) \in (s(1,t),2) \times (0,1), \tag{4.6c}$$

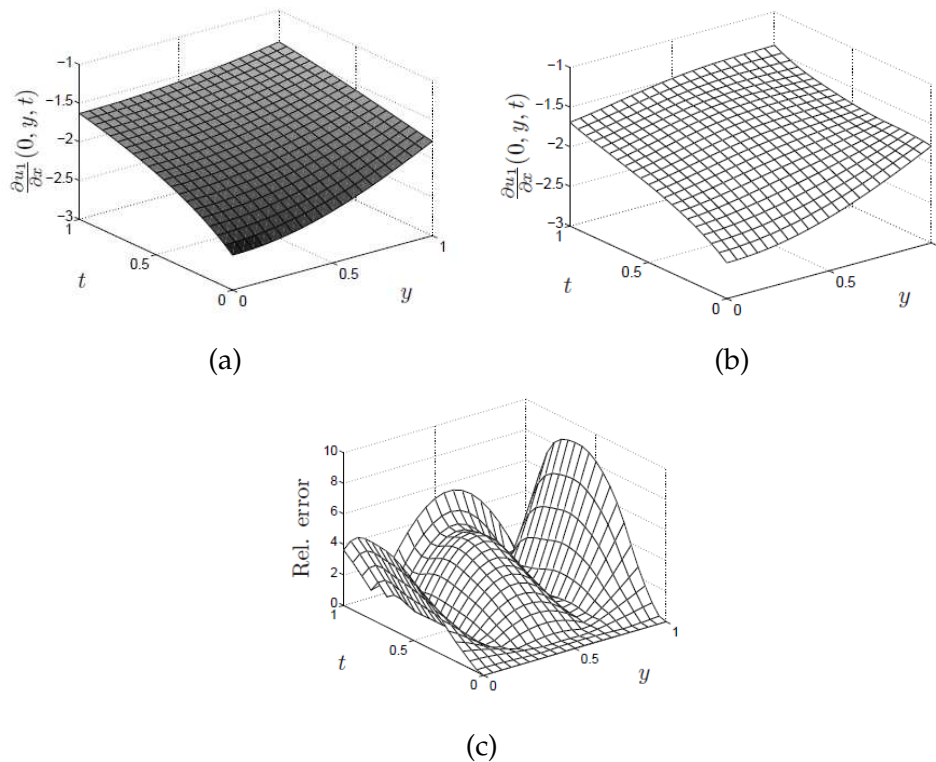


Figure 9: (a) The exact heat flux, (b) the MFS approximation, and (c) the relative error (%), on the boundary $x=0$, obtained with $h_1=h_2=2$, for Example 2 (no noise).

where $\gamma=0.479611$, $t^0=0.695571$, and erf and erfc are the error and complementary error functions, respectively, given by

$$\operatorname{erf}(\xi) = \frac{2}{\sqrt{\pi}} \int_0^\xi e^{-\sigma^2} d\sigma \quad \text{and} \quad \operatorname{erfc}(\xi) = 1 - \operatorname{erf}(\xi).$$

The initial data (2.4a) and (2.4b) are given by

$$u_1(x, y, 0) = u_1^0(x, y) = 1 - \frac{\operatorname{erf}\left(\frac{x-y}{\sqrt{8\alpha_1 t^0}}\right)}{\operatorname{erf}\left(\frac{\gamma}{\sqrt{8\alpha_1}}\right)},$$

$$(x, y) \in \Omega_1(0) = \{(x, y) \in \mathbb{R}^2 \mid y \in (0, 1), x \in (0, s(y, 0))\}, \quad (4.7a)$$

$$u_2(x, y, 0) = u_2^0(x, y) = -1 + \frac{\operatorname{erfc}\left(\frac{x-y}{\sqrt{8\alpha_2 t^0}}\right)}{\operatorname{erfc}\left(\frac{\gamma}{\sqrt{8\alpha_2}}\right)},$$

$$(x, y) \in \Omega_2(0) = \{(x, y) \in \mathbb{R}^2 \mid y \in (0, 1), x \in (s(y, 0), 2)\}. \quad (4.7b)$$

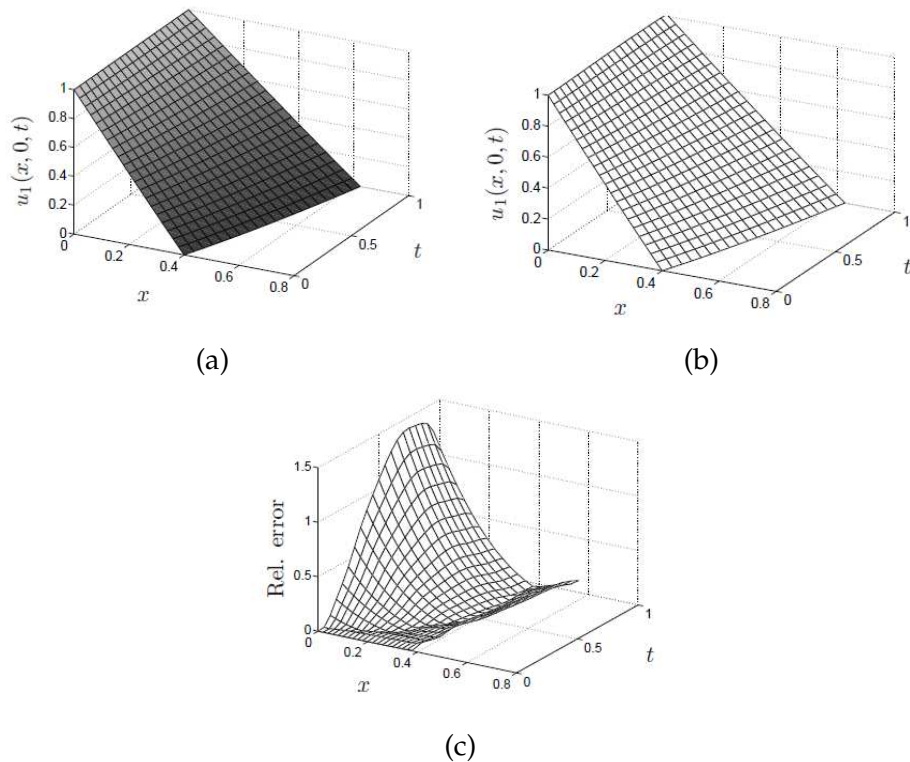


Figure 10: (a) The exact temperature solution, (b) the MFS approximation, and (c) the relative error (%), on the boundary $y=0$, obtained with $h_1=h_2=2$, for Example 2 (no noise).

Note that the inward unit normal to the interface boundary $\Sigma = \{(x, y, t) \in \mathbb{R}^3 \mid y \in (0, 1), t \in (0, 1), x = s(y, t)\}$ is given by

$$v = -\frac{\nabla\Phi}{|\nabla\Phi|} = \frac{1}{\sqrt{2}}(-1, 1),$$

where $\Phi(x, y, t) = x - s(y, t)$. Then the problem given by the Eqs. (2.1)-(2.5), with the data (4.5)-(4.7b) has the analytic solution

$$u_1(x, y, t) = 1 - \frac{\operatorname{erf}\left(\frac{x-y}{\sqrt{8\alpha_1(t+t^0)}}\right)}{\operatorname{erf}\left(\frac{\gamma}{\sqrt{8\alpha_1}}\right)},$$

$$(x, y, t) \in \overline{\Omega}_1 = \{(x, y, t) \in \mathbb{R}^3 \mid y \in [0, 1], t \in [0, 1], x \in [0, s(y, t)]\}, \quad (4.8a)$$

$$u_2(x, y, t) = -1 + \frac{\operatorname{erfc}\left(\frac{x-y}{\sqrt{8\alpha_2(t+t^0)}}\right)}{\operatorname{erfc}\left(\frac{\gamma}{\sqrt{8\alpha_2}}\right)},$$

$$(x, y, t) \in \overline{\Omega}_2 = \{(x, y, t) \in \mathbb{R}^3 \mid y \in [0, 1], t \in [0, 1], x \in [s(y, t), 2]\}. \quad (4.8b)$$

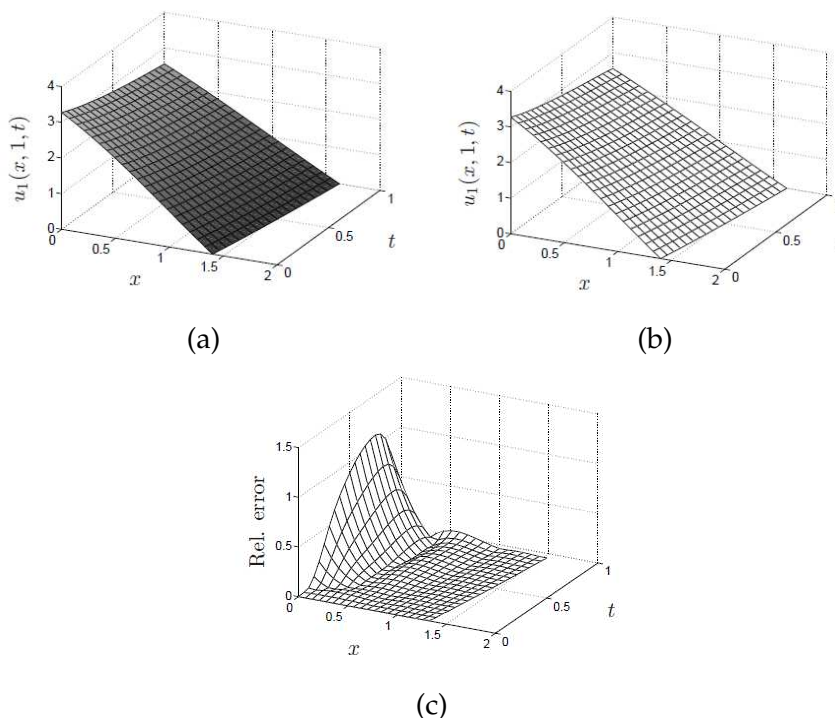


Figure 11: (a) The exact temperature solution, (b) the MFS approximation, and (c) the relative error (%), on the boundary $y=1$, obtained with $h_1=h_2=2$, for Example 2 (no noise).

The unknown data which is sought is given by the temperature u_1 on Γ_1 and the heat flux $\partial u_1/\partial \nu$ on the left wall $x=0$, namely

$$u_1(0,y,t) = 1 - \frac{\operatorname{erf}\left(-\frac{y}{\sqrt{8\alpha_1(t+t^0)}}\right)}{\operatorname{erf}\left(\frac{\gamma}{\sqrt{8\alpha_1}}\right)}, \tag{4.9a}$$

$$\frac{\partial u_1}{\partial x}(0,y,t) = -\frac{\sqrt{2}}{2} \frac{\exp\left(-\frac{(x-y)^2}{8\alpha_1(t+t^0)}\right)}{\sqrt{\pi\alpha_1(t+t^0)}\operatorname{erf}\left(\frac{\gamma}{\sqrt{8\alpha_1}}\right)}, \quad (y,t) \in (0,1) \times (0,1), \tag{4.9b}$$

$$u_1(x,0,t) = 1 - \frac{\operatorname{erf}\left(\frac{x}{\sqrt{8\alpha_1(t+t^0)}}\right)}{\operatorname{erf}\left(\frac{\gamma}{\sqrt{8\alpha_1}}\right)}, \quad (x,t) \in (0,s(0,t)) \times (0,1), \tag{4.9c}$$

$$u_1(x,1,t) = 1 - \frac{\operatorname{erf}\left(\frac{x-1}{\sqrt{8\alpha_1(t+t^0)}}\right)}{\operatorname{erf}\left(\frac{\gamma}{\sqrt{8\alpha_1}}\right)}, \quad (x,t) \in (0,s(1,t)) \times (0,1). \tag{4.9d}$$

In order to test the stability of the numerical results noise is added to the temperature

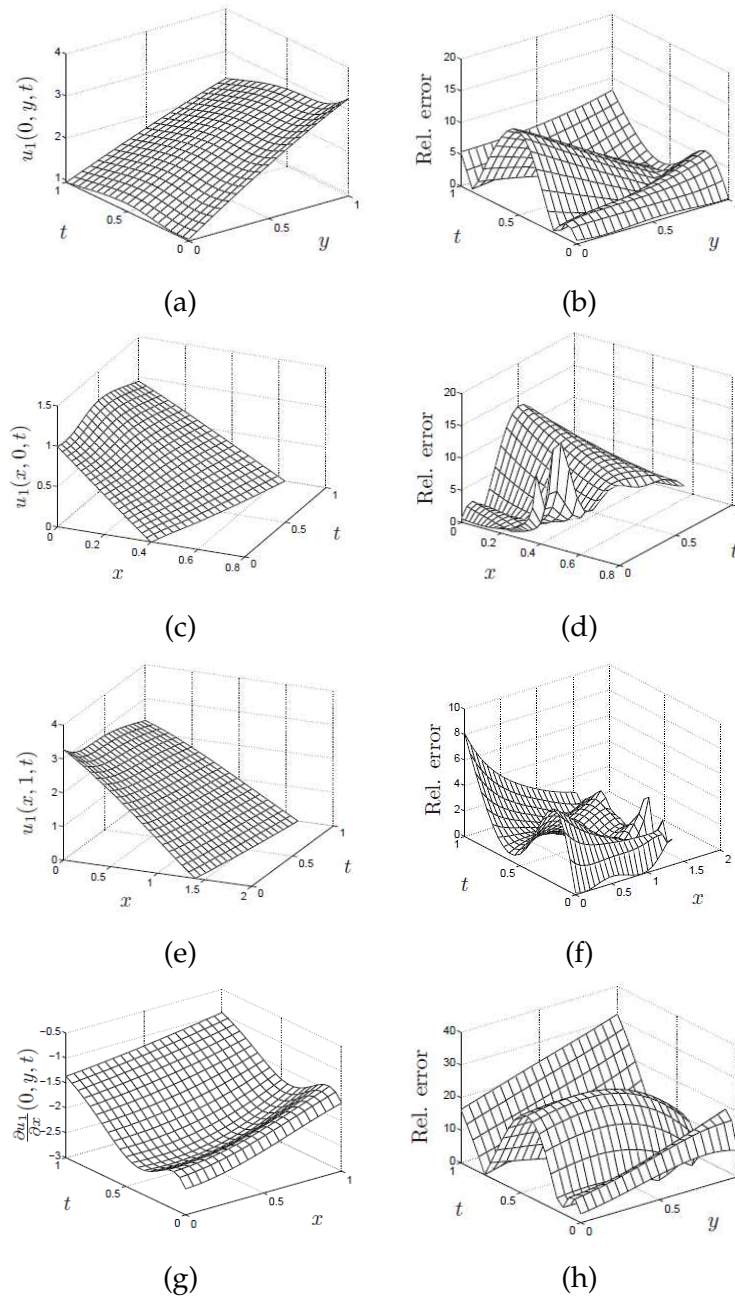


Figure 12: The MFS approximation of the temperature on (a) $x=0$, (c) $y=0$, (e) $y=1$ and the MFS approximation of the flux on (g) $x=0$, and the relative error (%) between the exact and numerical $u_1(x,y,t)$ on (b) $x=0$, (d) $y=0$, (f) $y=1$, and (h) the relative error (%) between the exact and numerical $(\partial u_1 / \partial x)(0,y,t)$, obtained with $h_1=h_2=2$, for Example 2 ($p=5\%$ noise).

data (2.3), via (4.6a)-(4.6c), as in (4.4). When $p = 0$ and $p = 5\%$, we use $\lambda = 10^{-13}$ and $\lambda = 10^{-6}$, respectively. The numerical results are presented in Figs. 8-12 and the same conclusions as in Example 1 are obtained.

4.3 Example 3

We consider $T = 1, K_1 = 1, K_2 = 2, \alpha_1 = 2, \alpha_2 = 1, l = \pi/2$. We take the moving boundary as in [1], given by

$$s(y,t) = \tan^{-1}(y^2 + t + 1), \quad (y,t) \in (0,1) \times (0,1), \tag{4.10a}$$

$$u_2(x,y,0) = u_2^0(x,y) = (\tan^{-1}(y^2 + 1) - x)^2 |\cos(2y)|, \\ (x,y) \in \Omega_2(0) = \{(x,y) \in \mathbb{R}^2 | y \in (0,1), x \in (s(y,0), \pi/2)\}. \tag{4.10b}$$

We also take

$$u_2 = f = u_2^0 + t \quad \text{on } \Gamma_2. \tag{4.11}$$

In [1], the initial condition (2.4a) was also imposed as in (4.10b) and the numerical results were found meaningless probably because the resulting inverse problem has no solution.

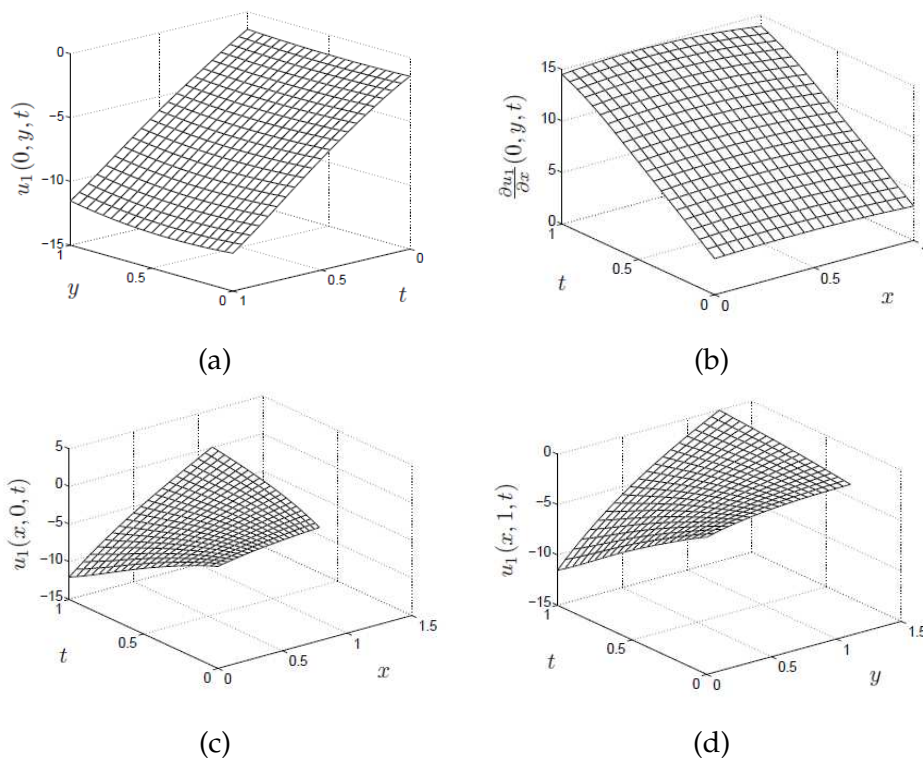


Figure 13: The MFS approximations for: (a) $u_1(0,y,t)$, (b) $\partial u_1 / \partial x(0,y,t)$, (c) $u_1(x,0,t)$, and (d) $u_1(x,1,t)$, obtained with $h_1 = 4$ and $h_2 = 2$, for Example 3 (no noise).

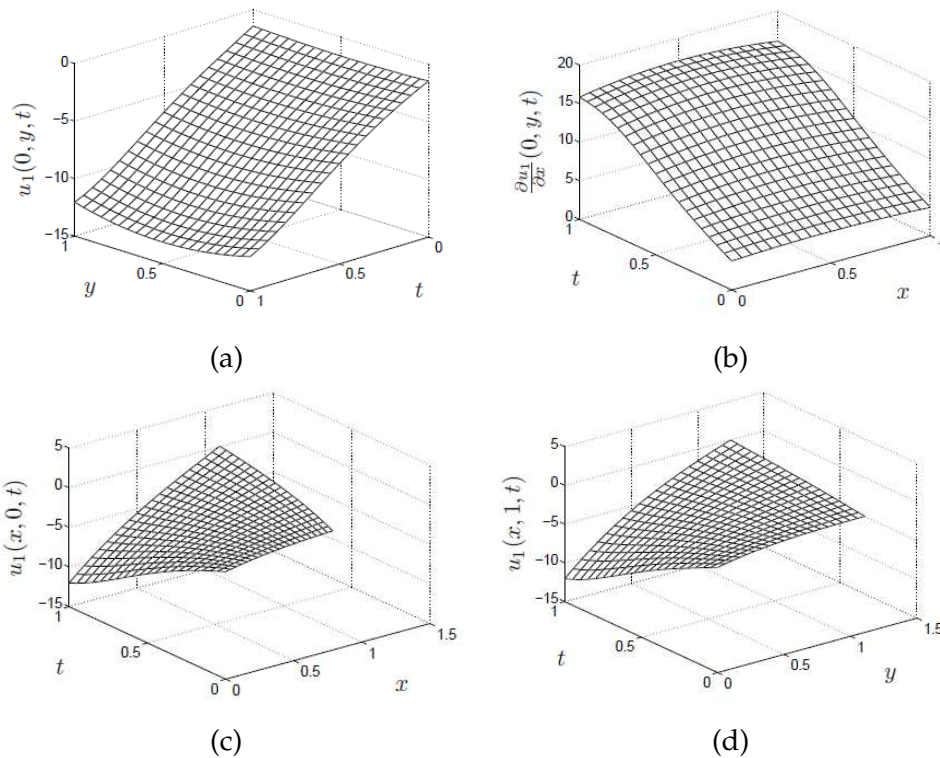


Figure 14: The MFS approximations for: (a) $u_1(0,y,t)$, (b) $\partial u_1/\partial x(0,y,t)$, (c) $u_1(x,0,t)$, and (d) $u_1(x,1,t)$, obtained with $h_1=3$ and $h_2=2$, for Example 3 ($p=5\%$ noise).

In our study, we do not impose the initial condition (2.4a) in the inverse problem. In this case, the system of Eqs. (3.3) contains $2M_3(M_1+1)+N_1(M_1+(M_2+1)/2)$ equations with $4MN$ unknowns. Taking $M_1=20$, $M_2=20$, $M_3=10$, $N_1=40$, $M=10$, $N=40$, we obtain a system of 1640 equations with 1600 unknowns.

Example 3 has no analytical solution available explicitly. Plots of the MFS approximations obtained for $p=0$ (and $\lambda=10^{-7}$) and $p=5\%$ (and $\lambda=10^{-6}$) are shown in Figs. 13 and 14, respectively. Further, the values of the mean and maximum absolute differences between the MFS approximations obtained for $p=0$ and $p=5\%$ are shown in Table 1. From Figs. 13 and 14, and Table 1 it can be seen that the differences between the numerical results are of the same order as the amount of noise. Furthermore, the numerical solution in Fig. 14 is stable, free of oscillations and unbounded behaviour.

Table 1: Mean and maximum differences between the MFS approximations obtained for $p=0$ and 5%, for Example 3.

Figures to compare	13(a) & 14(a)	13(b) & 14(b)	13(c) & 14(c)	13(d) & 14(d)
Mean difference	0.3197	1.0413	0.0740	0.0860
Max difference	0.6380	1.9025	0.5886	0.5808

5 Conclusions

We have extended the MFS of [11] to the inverse two-phase two-dimensional linear Stefan problem. The numerical results show that the method is accurate and stable with respect to noise in the input data. Future work will concern extending the MFS developed in this study to the three-phase and three-dimensional inverse Stefan problems, see [17, 18], respectively.

Acknowledgments

T. Reeve would like to acknowledge the financial support received from the EPSRC.

References

- [1] D. D. ANG, A. PHAM NGOC DINH AND D. N. THANH, *Regularization of a two-dimensional two-phase inverse Stefan problem*, *Inverse Problems*, 13 (1997), pp. 607–619.
- [2] J. B. BELL, *The noncharacteristic Cauchy problem for a class of equations with time dependence, II*, *SIAM J. Math. Anal.*, 12 (1981), pp. 778–797.
- [3] C. S. CHEN, H. A. CHO AND M. A. GOLBERG, *Some comments on the ill-conditioning of the method of fundamental solutions*, *Eng. Anal. Boundary Elements*, 30 (2006), pp. 405–410.
- [4] D. COLTON, *The inverse Stefan problem for the heat equation in two space variables*, *Mathematika*, 21 (1974), pp. 282–286.
- [5] D. COLTON AND R. REEMTSMA, *The numerical solution of the inverse Stefan problem in two space variables*, *SIAM J. Appl. Math.*, 44 (1984), pp. 996–1013.
- [6] N. L. GOL'DMAN, *Inverse Stefan Problems*, Kluwer Academic Publ., Dordrecht, 1997.
- [7] P. C. HANSEN, *Analysis of discrete ill-posed problems by means of the L-curve*, *SIAM Rev.*, 34 (1992), pp. 561–580.
- [8] DINH NHO HÀO, *Methods for Inverse Heat Conduction Problems*, Peter Lang, Frankfurt am Main, 1998.
- [9] C. D. HILL, *Parabolic equations in one space variable and the non-characteristic Cauchy problem*, *Commun. Pure Appl. Math.*, 20 (1967), pp. 619–633.
- [10] B. T. JOHANSSON AND D. LESNIC, *A method of fundamental solutions for transient heat conduction in layered materials*, *Eng. Anal. Boundary Elements*, 33 (2009), pp. 1362–1367.
- [11] B. T. JOHANSSON, D. LESNIC AND T. REEVE, *A method of fundamental solutions for the two-dimensional inverse Stefan problem*, *Inverse Problems Sci. Eng.*, (submitted).
- [12] B. T. JOHANSSON, D. LESNIC AND T. REEVE, *A method of fundamental solutions for two-dimensional heat conduction*, *Int. J. Comput. Math.*, 88 (2011), pp. 1697–1713.
- [13] B. T. JOHANSSON, D. LESNIC AND T. REEVE, *A meshless method for an inverse two-phase one-dimensional linear Stefan problem*, *Inverse Problems Sci. Eng.*, 21(1) (2013), pp. 17–33.
- [14] A. KARAGEORGHIS, D. LESNIC AND L. MARIN, *A survey of applications of the MFS to inverse problems*, *Inverse Problems Sci. Eng.*, 19 (2011), pp. 309–336.
- [15] P. A. RAMACHANDRAN, *Method of fundamental solutions: singular value decomposition analysis*, *Commun. Numer. Methods Eng.*, 18 (2002), pp. 789–801.

- [16] L. RUBINSTEĪN, *The Stefan problem: comments on its present state*, J. Inst. Maths Applics, 24 (1979), pp. 259–277.
- [17] D. SLOTA, *Using genetic algorithms for the determination of an heat transfer coefficient in three-phase inverse Stefan problem*, Int. Commun. Heat Mass Transfer, 35 (2008), pp. 149–156.
- [18] D. SLOTA, *Identification of the cooling condition in 2-D and 3-D continuous casting processes*, Numer. Heat Trans. B, 55 (2009), pp. 155–176.